Supplementary information for

Structure design of cubic Sr,V:$CeFeO_3$ thin films with strong magneto-optical effect and high compatibility with Si substrate

Nanxi Lin,[a,b] Shengnan Zhang,[a,b] Haixin Chen,[a,b] Yunjin Chen,[a,b,c] Xin Chen,[a,b] Yongfan Zhang,[a] Xiaolin Hu,*[a,b] and Naifeng Zhuang*[a,b]

[a]College of Chemistry, Fuzhou University, Fuzhou 350108, China.

[b]Institute of Optical Crystalline Materials, Fuzhou University, Fuzhou 350108, China.

[c]Fuzhou BOE Optoelectronics Technology Co., Ltd. Fuzhou 350300, China.

Email: linamethyst@fzu.edu.cn (X. Hu), nfzhuang@fzu.edu.cn (N. Zhuang)

1. Sputtering apparatus

The series of $Ce_{1-x}Sr_xFe_{1-x}V_xO_3$ (x=0.3, 0.5, 0.7) thin films were prepared by using radio frequency magnetron sputtering method. The sketch of vacuum sputtering cavity is shown in Fig. S1. The cavity is filled with Ar gas. Under an electric field (E), the electrons produced from argon ionization move quickly to the substrate. As they move, the electrons collide with the remaining argon atoms, and then the argon atoms are ionized into Ar^+ ions and new electrons are released. The new electrons also move to the substrate. Meanwhile, the Ar+ ions with high energy accelerate towards the cathode target, and hit the target surface to make it sputter. And then the sputtered target material atoms move toward the anode electrode and deposit on the substrate to form a thin film. It's worth mentioning that the magnetron sputtering method can significantly increase the sputtering rate by introducing a magnetic field at the cathode electrode. The magnetic field is used to restrain the charged particles to increase the plasma density to increase the sputtering rate. Additionally, this method has the advantages of being suitable for large-scale industrial production because a large sputtering

area can be implemented and the deposition of thin film can be accurately controlled.

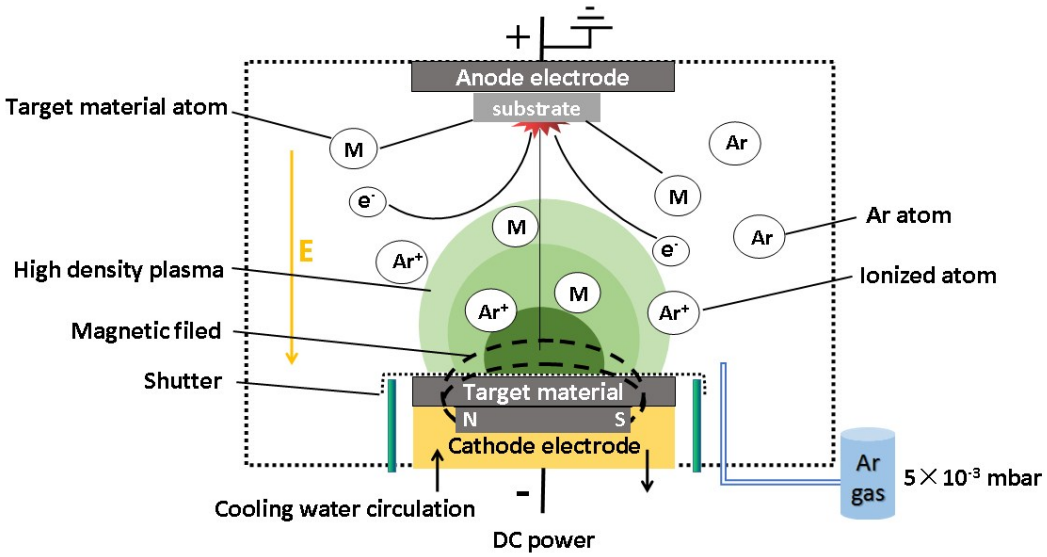

Fig. S1. The sketch of vacuum sputtering cavity.

2. Structure parameters

To further understand the crystal structure, the structure refinement of $Ce_{1-x}Sr_xFe_{1-x}V_xO_3$/Si ($x$=0.3, 0.5, 0.7) thin films were carried out based on the Rietveld principle with the crystal structure of cubic perovskite $LaSrFeVO_6$ as the basic model. The structure parameters such as the atomic position and the occupancy rate of thin films are listed in Table S1.

Table S1. The structure parameters of $Ce_{1-x}Sr_xFe_{1-x}V_xO_3$.

Chemical formula	Atom	Wyckoff-site	*x*	*y*	*z*	Occupancy
$Ce_{0.3}Sr_{0.7}Fe_{0.3}V_{0.7}O_3$	Ce1	8c	0.25	0.25	0.25	0.3
	Sr1	8c	0.25	0.25	0.25	0.7
	Fe1	4a	0	0	0	0.39
	Fe2	4b	0.5	0.5	0.5	0.21
	V1	4a	0	0	0	0.49
	V2	4b	0.5	0.5	0.5	0.91
	O1	24e	0.258(3)	0	0	1
$Ce_{0.5}Sr_{0.5}Fe_{0.5}V_{0.5}O_3$	Ce1	8c	0.25	0.25	0.25	0.5
	Sr1	8c	0.25	0.25	0.25	0.5
	Fe1	4a	0	0	0	0.65
	Fe2	4b	0.5	0.5	0.5	0.35
	V1	4a	0	0	0	0.35
	V2	4b	0.5	0.5	0.5	0.65
	O1	24e	0.252(4)	0	0	1
$Ce_{0.7}Sr_{0.3}Fe_{0.7}V_{0.3}O_3$	Ce1	8c	0.25	0.25	0.25	0.7
	Sr1	8c	0.25	0.25	0.25	0.3
	Fe1	4a	0	0	0	0.91
	Fe2	4b	0.5	0.5	0.5	0.49
	V1	4a	0	0	0	0.21
	V2	4b	0.5	0.5	0.5	0.39
	O1	24e	0.247(5)	0	0	1

3. Theoretical calculation

XRD patterns, GIXRD patterns and the results of Rietveld refinement show $Ce_{1-x}Sr_xFe_{1-x}V_xO_3$ thin films have the periodic crystal structures. In order to discuss the magneto-optical enhancement mechanism of $Ce_{1-x}Sr_xFe_{1-x}V_xO_3$ thin films, the partial density of states (PDOS) of $Ce_{1-x}Sr_xFe_{1-x}V_xO_3$ were calculated by using the density functional theory (DFT) based on pseudopotential plane wave. (B. Li, A. Michaelides, and M. Scheffler, *Phys. Rev. B*, 2007, 76, 075401; M. C. Payne, M. P. Teter, D. C. Allan, T. A. Arias, and J. D. Joannopoulos, *Rev. Mod. Phys.*, 1992, 64, 1045; M. Bochstedte, A. Kley, J. Neugebauer, and M. Scheffler, *Comput. Phys. Commun.*, 1997, 107, 187) The pseudopotential plane wave method is suitable for periodic structure. (H.W. Kunert, *Eur. Phys. J. Appl. Phys.*, 2004, 27, 251–254.) All of DFT calculations were performed with Cambridge Sequential Total Energy Package (CASTEP) program package in Materials Studio software. (N. Daldosso et al., *Phys. Rev. B*, 2003, 68, 085327; S. J. Clark, M. D. Segall, C. J. Pickard, P. J. Hasnip, M. I. J. Probert, K. Refson, and M. C. Payne, Z. Kristallogr. 2005, 220, 567; M. D. Segall, P. L. D. Lindan, M. J. Probert, C. J. Pickard, P. J. Hasnip, S. J. Clark, and M. C. Payne, *J. Phys.: Condens. Matter*, 2002, 14, 2717) The models of $Ce_{1-x}Sr_xFe_{1-x}V_xO_3$ (x=0.3, 0.5, 0.7) have been built based on the results of Rietveld refinement, as shown in Fig. 4. In order to calculate accurately, the generalized gradient approximation (GGA) with Perdew-Burke-Ernzerhof (PBE) type exchange-correlation functions was adopted to treat the perovskite-type rare earth ferrite. (N. Lin, Y. Wang, Y. Zhao, L. Huo, W. Shi, X. Chen, Y. Zhang, X. Hu, and N. Zhuang, *Ceram. Int.*, 2019, 45,14928-14933; J. P. Perdew, K. Burke, and M. Ernzerhof, *Phys. Rev. Lett.*, 1996, 77, 3865; J. P. Perdew, K. Burke, and M. Ernzerhof, *Phys. Rev. Lett.*, 1997, 78, 1396) The plane wave basis sets are used with the ultrasoft pseudopotential. The Monkhorst-Pack grid k-points of 2×2×2, the energy cutoff of 330.0 eV, the SCF tolerance of 2.0×10^{-6} eV/atom were adopted.

4. Cross-section morphology

The scanning electron microscope (SEM) (SU8000, Hitachi, Japan) was used to measure the cross section morphology of thin films. As shown in Fig. S2, the $Ce_{0.5}Sr_{0.5}Fe_{0.5}V_{0.5}O_3$ thin film grew in Volmer-Weber growth mode and its thickness is about 349 nm when the sputtering time of 1.5 hours is insufficient. For the film sputtered for 3 hours, the thickness reaches about 578 nm. The film has fewer grain boundaries and higher crystallinity. This indicates that the quality of thin film has been improved. Therefore, in this paper, the sputtering time of 3 hours is selected to prepare the series of $Ce_{1-x}Sr_xFe_{1-x}V_xO_3$ films.

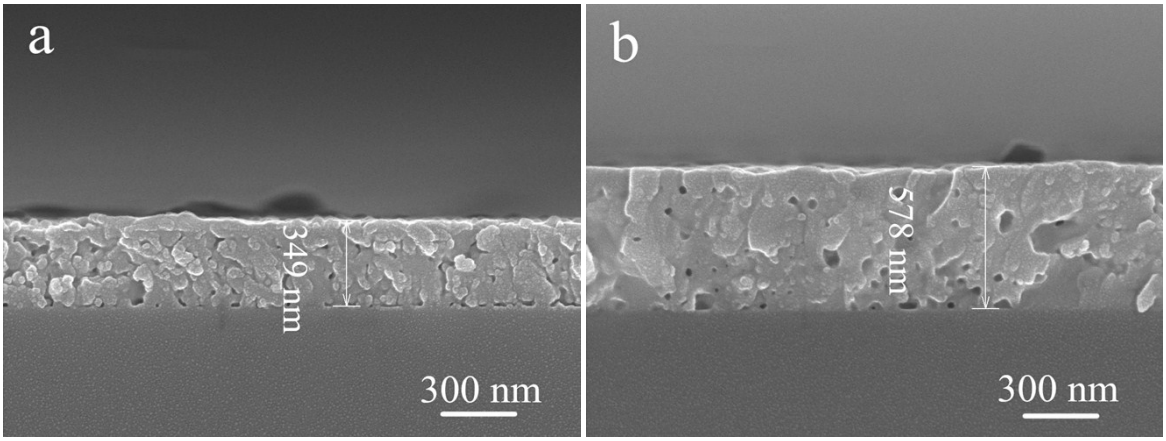

Fig. S2. SEM image of $Ce_{0.5}Sr_{0.5}Fe_{0.5}V_{0.5}O_3$/Si thin film in cross-section. Deposition time is (a) 1.5 hours and (b) 3 hours.

5. XPS spectra

The survey scan XPS spectra for $Ce_{1-x}Sr_xFe_{1-x}V_xO_3$/Si thin films are shown in Fig. S3, which indicates the presence of Ce, Sr, Fe, V, and O elements. The peak-fitting of each element (Fig. 5a-e) and the more discussions in detail are shown in the main manuscript.

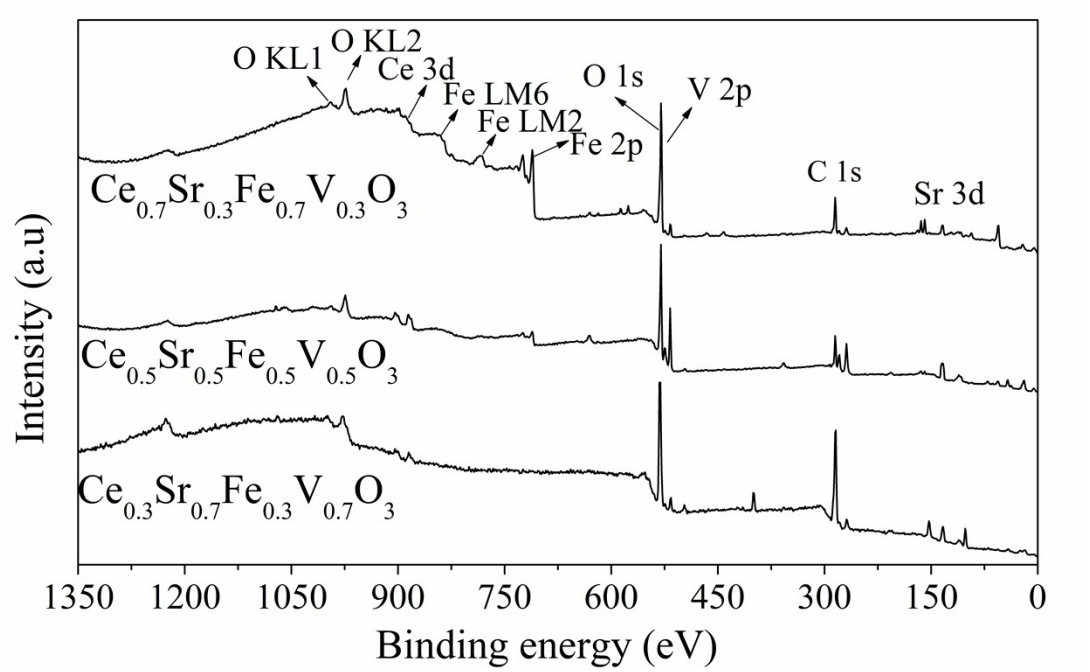

Fig. S3. Survey scan XPS spectra of $Ce_{1-x}Sr_xFe_{1-x}V_xO_3$/Si.

6. Morphology of $Ce_{1-x}Sr_xFe_{1-x}V_xO_3$/STO

The AFM images of the surface morphology of $Ce_{1-x}Sr_xFe_{1-x}V_xO_3$/STO thin films are shown in Fig. S4. As can be seen from the AFM images, the grain size and the grain distribution of thin films are uniform, and the surfaces are smooth and crack-free. The RMS roughness (Rq) of these thin films are all below 10 nm, indicating that this series of films have good quality.

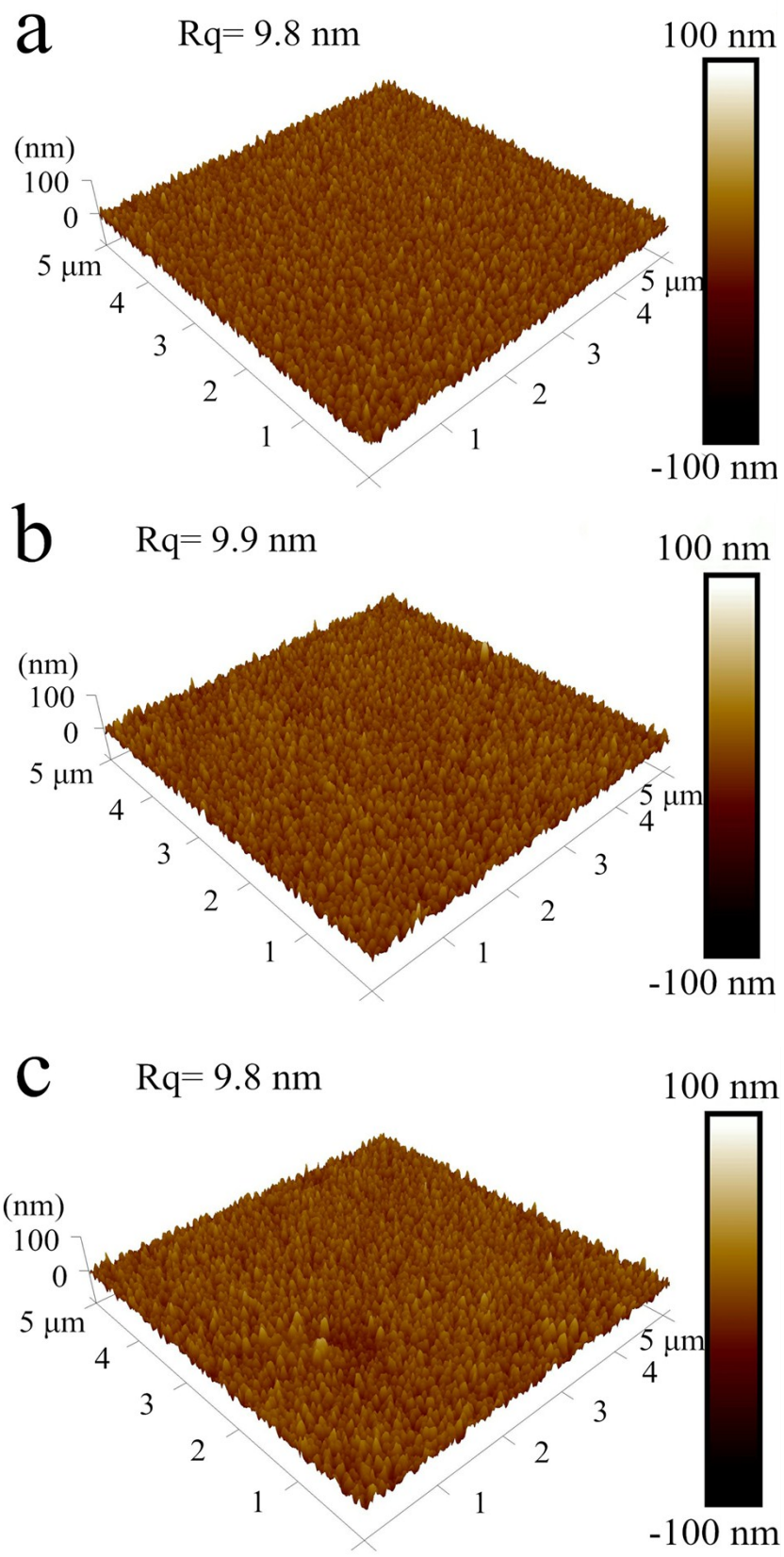

Fig. S4. AFM images of (a) $Ce_{0.3}Sr_{0.7}Fe_{0.3}V_{0.7}O_3$/STO, (b) $Ce_{0.5}Sr_{0.5}Fe_{0.5}V_{0.5}O_3$/STO, and (c) $Ce_{0.7}Sr_{0.3}Fe_{0.7}V_{0.3}O_3$/STO thin films.

7. Crystalline phase of $Ce_{1-x}Sr_xFe_{1-x}V_xO_3$/STO

In order to observe the intrinsic transmittance of $Ce_{1-x}Sr_xFe_{1-x}V_xO_3$ thin films and exclude the absorption interference of Si substrate, the <111>-oriented $SrTiO_3$ (STO) crystal were used as the substrate. Fig. S5a shows the GIXRD patterns of annealed $Ce_{1-x}Sr_xFe_{1-x}V_xO_3$/STO ($x$=0.3, 0.5, 0.7) thin films. Compared with the diffraction card (JCPDS 54-0757), $Ce_{1-x}Sr_xFe_{1-x}V_xO_3$/STO thin films have the cubic perovskite structure. The diffraction peaks of $Ce_{0.7}Sr_{0.3}Fe_{0.7}V_{0.3}O_3$ thin film shift slightly to the lower angle when comparing to those of $Ce_{0.5}Sr_{0.5}Fe_{0.5}V_{0.5}O_3$ and $Ce_{0.3}Sr_{0.7}Fe_{0.3}V_{0.7}O_3$, which is consistent with the results of the Rietveld structure refinement (Table 2). The increased crystal cell parameters cause the diffraction peak to shift to the lower angle. In addition, only one diffraction peak attributed to (222) plane of cubic perovskite except those of STO substrate can be observed from Fig. S5b. Therefore, $Ce_{1-x}Sr_xFe_{1-x}V_xO_3$/STO thin films prefer to grow along the <111>-orientation.

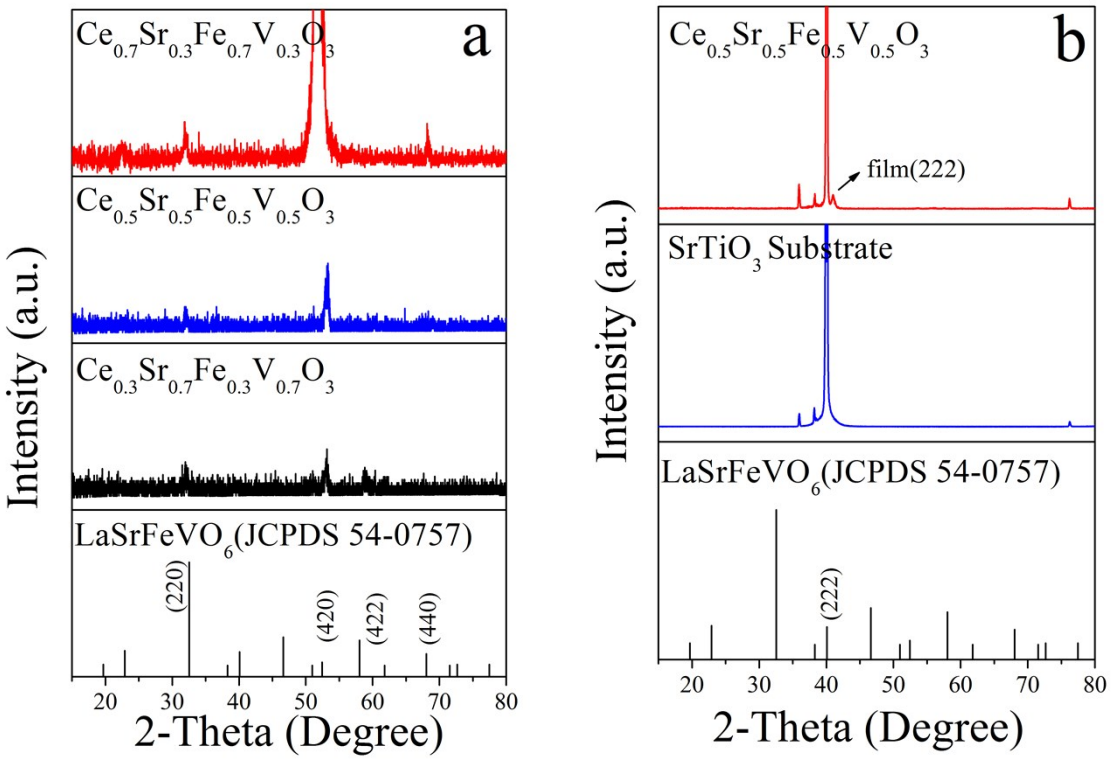

Fig. S5. (a) GIXRD patterns of annealed $Ce_{1-x}Sr_xFe_{1-x}V_xO_3$/STO thin films, (b) XRD pattern of $Ce_{0.5}Sr_{0.5}Fe_{0.5}V_{0.5}O_3$ thin film.

8. Transmittance

The optical transmittance of thin film has a certain influence on its practical applications. The UV-Vis-IR spectrometer (PerkinElmer Lambda 900, Waltham, MA, USA) was used to measure the transmittance spectra of thin films in the wavelength range of 200-3000 nm. As shown in Fig. S6a, the transmittance of $Ce_{1-x}Sr_xFe_{1-x}V_xO_3$/Si thin films is about 60-70 % in the range of 1500-3000 nm. Moreover, the transmittance of film is affected by the surface roughness. The lower the roughness, the higher the transmittance. It also can be seen from Fig. S6a that the absorption edge of Si substrate is about 1000 nm. The intrinsic transmittance of $Ce_{1-x}Sr_xFe_{1-x}V_xO_3$ thin films can be observed if the $SrTiO_3$ (STO) crystal is used as the substrate. As shown in Fig. S6b, the intrinsic transmittance of $Ce_{1-x}Sr_xFe_{1-x}V_xO_3$ thin films is about 65-75 % within 800-3000 nm. These indicate that $Ce_{1-x}Sr_xFe_{1-x}V_xO_3$ thin films have sufficient transmittance and can be applied to magneto-optical devices in near-infrared region.

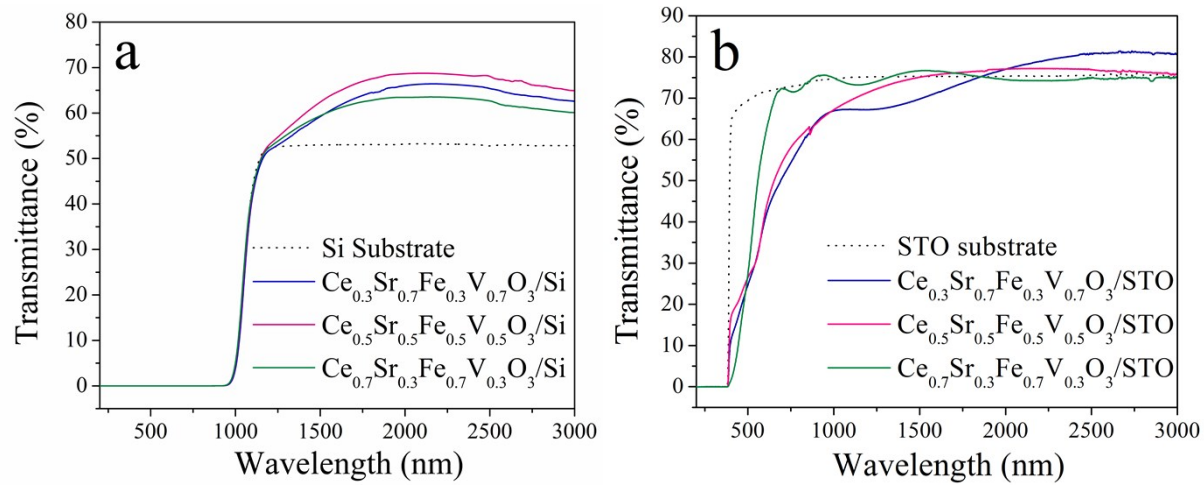

Fig. S6. The transmittance spectra of $Ce_{1-x}Sr_xFe_{1-x}V_xO_3$ thin films deposited on (a) Si and (b) STO substrates.